THE ASTROPHYSICAL JOURNAL, 246:444–454, 1981 June 1

SPECTROPOLARIMETRY AND THE PHYSICAL STRUCTURE OF PROTO-PLANETARY NEBULAE

GARY D. SCHMIDT[1]
Lick Observatory, University of California, Santa Cruz; and
Department of Astronomy, University of Minnesota

AND

MARTIN COHEN[2]
NASA Ames Research Center, Moffett Field, California
Received 1980 November 17; accepted 1980 December 8

ABSTRACT

Optical spectropolarimetry and spectrophotometry are presented of the two bipolar nebulae GL 618 and M2-9. A comparison of the polarization in the emission lines and the continuum is used to construct geometrical and physical models for each object. We find that the forbidden lines arise largely in the visible nebulae, whereas the permitted lines are formed in a central high-density region and are scattered with the stellar continuum by dust grains in the lobes. Condensations are found to be an important component of the lobes, reinforcing the view that these bipolars represent a very early phase in the life of a planetary nebula.

Subject headings: nebulae: planetary — nebulae: reflection — polarization

I. INTRODUCTION

A continuing interest in bipolar nebulae by observers working in a variety of fields has resulted in the identification of several objects which bear characteristics thought to be indicative of very young planetary nebulae (or proto–PNs). Examples are M2-9 (Allen and Swings 1972), GL (CRL) 618 (Westbrook *et al.* 1975), M1-91 (Calvet and Cohen 1978), and M1-92 (Herbig 1975).

The bipolar appearance of these objects is a manifestation of our perspective and the distribution of a large quantity of dust around a star in an optically thick toroidal ring and a pair of polar lobes (Herbig 1975; Ney *et al.* 1975). The high degree of obscuration results in an overall spectrum dominated by thermal IR emission from the dust grains; the stellar component itself may be completely obscured in our direction at visual wavelengths. Optical spectra of the nebulosities usually display a reflected stellar continuum underlying a molecular and/or atomic emission-line spectrum which is biased in favor of low-ionization species as compared with normal PN spectra. The radio continua are typically weak and self-absorbed at low frequencies, but millimeter-wavelength spectra usually reveal CO in emission. Zuckerman (1978) and Zuckerman *et al.* (1977, 1978) interpret this fact, together with a strong tendency for the objects to have an abundance ratio $C/O > 1$, as indications for a post–carbon star evolutionary status. A general review of the optical, IR, and radio continuum properties of several bipolar nebulae in an evolutionary context has been presented by Calvet and Cohen (1978).

Detailed analyses of the nebular spectra of these objects are complicated by several factors. First, stratification of the emission-line zones is apparent on optical photographs of the larger objects as well as from inspection of relative line strengths. The large degree of obscuration necessitates substantial reddening corrections; furthermore, the extinction may be distributed nonuniformly over the objects. If the dust coexists with the emitting gas, it can affect the ionization structure of the nebulae through absorption and scattering of UV photons. A significant degree of scattering in the optical will also confuse the data by intermixing spectra from different regions.

Measurements of linear polarization throughout the spectrum would permit an evaluation of the latter effect, since the scattered features will in general appear linearly polarized. The geometry of bipolar nebulae is known to be favorable for the production of polarization by scattering (Schmidt, Angel, and Beaver 1978), so such measurements should be practical for most of the strong spectral lines of bright objects. An evaluation of the importance of scattering may in turn permit an estimate of the effect dust has in defining the ionization structure of a particular nebula, as well as facilitate the study of emission regions which are hidden from view directly.

In this paper we discuss new observations of the optical spectral flux and polarization of the bipolar nebulae GL 618 and M2-9. The differing polarization properties of the continuum and emission lines are used to construct models for both objects. The inferred physical structure reinforces the view that these bipolars represent early phases in the evolution of planetary nebulae.

[1] Now at the University of Minnesota, Department of Astronomy.
[2] NAS/NRC Senior Postdoctoral Associate.

II. GL 618

GL 618 is a compact bipolar nebula identified by Westbrook *et al.* (1975) from a comparison of optical photographs with the AFGL catalog. Infrared photometry and spectroscopy by these authors and Kleinmann *et al.* (1978) reveal that the bulk of the emission arises in a small ($\sim 0''.4$) dust cloud of temperature ~ 250 K. The presence of very large broad-band polarization implies a substantial dust content for the lobes as well, while optical spectrophotometry reveals a peculiar low-ionization emission-line spectrum rich in [Fe II]. Westbrook *et al.*'s proposal that GL 618 is a PN in the formative stages received support from Gottlieb and Liller (1976), who reported an increase of 2.5 mag in photographic brightness over the past 30 years. The CO emission profile obtained by Lo and Bechis (1976) indicates the presence of a molecular cloud expanding with a velocity ~ 20 km s^{-1}. A small, self-absorbed radio continuum source surrounding the star has also been detected (Wynn-Williams 1977).

a) *Observations*

Observations of GL 618 were obtained during 1979 December with the Lick Observatory 3 m Shane telescope and image-tube scanner (ITS) operating as a spectropolarimeter (Miller, Robinson, and Schmidt 1980). In this mode, spectral flux and polarization information are obtained simultaneously, with a resolution equal to that of the standard configuration (10 Å for the grating used). Coverage of the wavelength range $\lambda\lambda$3750–7050 was obtained in two grating tilts for the eastern (brighter) nebulosity, while only the red tilt $\lambda\lambda$4700–7050 was used for the western lobe. The small nebulae were contained entirely within the 4''.0 circular diaphragms.

The spectrophotometry was reduced to units of flux per unit wavelength above the Earth's atmosphere using observations of stars calibrated by Stone (1977). The instrumental efficiency of measuring polarization was determined from observations made through a Polaroid filter, while position angles were tied to the equatorial system using measurements of interstellar polarization standard stars.

The observed Balmer decrements indicate a substantial, but identical, reddening of the emission-lines from the two lobes. Since the nebulae appear unequal in size and brightness, this fact suggests that the extinction toward GL 618 is primarily interstellar, rather than local, in nature (see also § IIc). We have therefore applied an extinction correction to the spectrophotometry following the interstellar relation formulated by Miller and Mathews (1972). The correction corresponds to $A_v = 3.5$ mag, which is identical to that adopted by Westbrook *et al.* (1975) on the basis of [S II] line ratios and continuum shape as well as the Balmer decrement.

The polarization and dereddened flux spectra for the east lobe of GL 618 are displayed in Figure 1. For plotting purposes only, the Stokes parameters of polarization have been smoothed by a rectangular running mean of width 30 Å. Representative $\pm 1\ \sigma$ error bars are shown throughout the polarization spectra; the width of the bars denotes the smoothing window. The spectral flux distribution is displayed at the original resolution.

A remarkable feature of the spectrum in Figure 1 is the enormous strength of the forbidden lines of neutral atoms. The intensity ratio [O I] λ6300/H$\alpha \approx 1$, nearly two orders of magnitude greater than that observed in a typical PN. Similarly, [N I] λ5200 is comparable in strength to Hβ, and the usually undetected lines Mg I] λ4571 and Na I $\lambda\lambda$5890, 5896 are quite prominent. The spectrum is rich in [Fe II] emission, and other lines of ionized species ([S II], [N II]) are moderately enhanced. Identifications and dereddened strengths relative to Hβ for lines which can be measured reliably are compiled for both lobes in Table 1.

The polarization spectra reveal a very strong continuum polarization ($\sim 25\%$) at a position angle of $\sim 0°$, and therefore confirm the general picture of illumination by a star located at the intersection of the east-west lobes. Changes in both degree of polarization and position angle are evident in most of the strong lines, but the polarization characteristics of the Balmer emission appear to differ from those of the forbidden lines. These results are discussed in detail below.

b) *The Central Star*

The dereddened continuum reflected in the lobes of GL 618 matches quite well the Rayleigh-Jeans tail of a relatively hot blackbody. Westbrook *et al.* (1975) and Calvet and Cohen (1978) have compared the observed flux of Hβ with the visual continuum in each lobe and estimate $T_* \approx 30{,}000$ K. A similar exercise, based on the lack of [O III] $\lambda\lambda$4959, 5007 (Kaler 1978) yields $T_* \lesssim 27{,}000$ K. These suggest a spectral type of $\sim$ B0. Of course, if dust with a strong wavelength dependence of absorption were present between the ionized gas and the star, these temperatures would be underestimates. However, radio continuum observations by Wynn-Williams (1977) imply a source $\sim 0''.15$ in diameter, smaller than the 0''.4 measured for the IR flux. We will adopt $T_* = 30{,}000$ K. The stellar luminosity is also uncertain, but Westbrook *et al.* point out that a luminosity in excess of the main-sequence value places the object at a considerable distance from the galactic plane. If GL 618 is a proto-PN, the main-sequence luminosity appropriate for a B0 spectral type ($2 \times 10^4\ L_\odot$) may itself be too large (Salpeter 1971). We will choose the main-sequence value, which implies a distance $D = 1.8$ kpc, but in view of the uncertainties in this parameter we will quote the distance dependence of quantities calculated below. The radius and volume of each lobe are $R_L \sim 4.0 \times 10^{16}$ (D/1.8 kpc) cm and $V_L \approx 2.7 \times 10^{50}$ (D/1.8 kpc)^3 cm^3.

c) *Geometry of the Emission Regions*

The optical depth due to scattering in the lobes can be estimated from the observed surface brightness of scattered radiation and the inferred flux incident on the particles (Schmidt, Angel, and Beaver 1978). Using the stellar parameters adopted above, $\tau_s \gtrsim 0.03$ (D/1.8 kpc)^2,

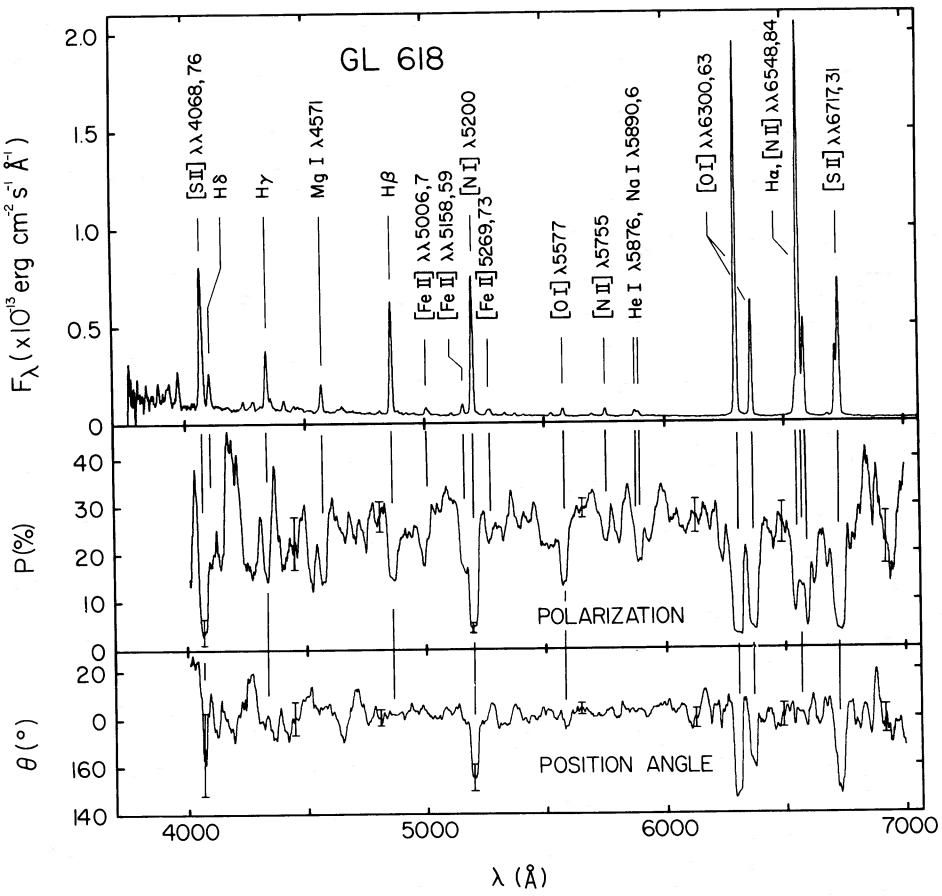

FIG. 1.—The polarization and de-reddened flux spectra of the east lobe of the bipolar nebula GL 618. Representative $\pm 1\ \sigma$ polarization error bars are shown; the widths indicate the smoothing window used (30 Å). A reduced emission-line polarization is apparent, with rotations in position angle also occurring in the very strong forbidden lines.

with the inequality resulting from the possible presence of extinction between the lobes and the star. Electrons as the scatterers are ruled out since the implied density in the lobes, $\langle N_e \rangle \gtrsim 5 \times 10^5$ cm^{-3}, would produce several orders of magnitude greater H I recombination radiation than is observed. The total mass in grains required to produce this optical depth is similar to that in the lobes of other bipolars ($\sim 10^{-4}\ M_\odot$) unless the dust is severely clumped.

A picture describing the geometry of the emission-line gas can be developed from a comparison of the polarization properties of lines from various ions. In Table 2 we summarize these properties by ion for both nebulosities. Stokes parameters of the underlying continuum have been subtracted from the line measurements, so the tabulated values are appropriate for the line radiation alone. However, some residual contamination due to Hα may be present in the measures for the [N II] doublet.

It is clear from an inspection of Table 2 that the emission lines of both lobes can be divided into two groups on the basis of their polarization characteristics: (1) the permitted lines (H I and He I), which exhibit the same position angle as the continuum, $\theta \approx 2°$, but a degree of polarization substantially reduced; and (2) the forbidden lines of heavy elements, with $P \approx 3\%$, $\theta \approx 140°$. A position angle of 140° in the equatorial system is nearly parallel to the galactic plane toward GL 618 (139°), so an interstellar origin for the forbidden-line polarization appears likely. Such a mechanism is confirmed by the data of Mathewson and Ford (1970), which reveal a region of strong, uniform polarization at $\theta \approx 150°$ in the vicinity $l^{II} = 166°$, $b^{II} = -7°$. We therefore conclude that the forbidden-line emission arises within the nebulous lobes themselves, and becomes polarized upon transmission through the intervening galactic medium. A polarization of 3% by interstellar mechanisms implies a considerable extinction as well, which substantiates our conclusion (§ II*a*) that the majority of the reddening toward GL 618 is interstellar in origin.

Since the permitted lines exhibit the same position angle as the continuum, we suppose that at least some fraction of this emission originates very near the star and is scattered in our direction by grains in the lobes. This

TABLE 1

DEREDDENED LINE INTENSITIES OF GL 618

IDENTIFICATION	EAST LOBE	WEST LOBE
Hβ(erg cm^{-2} s^{-1})	1.81×10^{-12}	5.55×10^{-13}
	Intensity Relative to Hβ = 100	
H8 λ3889	10	...
[Fe II] 8F λ3931 + CaII λ3934	25	...
Hε λ3971	31	...
[S II] λ4068, λ4076	152	...
Hδ λ4101	31	...
[Fe II] 21F λ4244, λ4245	7	...
[Fe II] 21F λ4277 + 7F λ4287	12	...
Fe II 32 λ4314 ?	5	...
Hγ λ4340 + [Fe II] 21F λ4347, λ4353, λ4358, + 7F λ4359	71	...
[Fe II] 7F λ4414 + 6F λ4415, λ4416	11	...
[Fe II] 6F λ4470 + 7F λ4475	15	...
Mg I] λ4571	28	...
[Fe II] 4F λ4640 + Fe II 43 λ4357	13	...
[Fe II] 20F λ4814	4	8
Hβ λ4861	100	100
[Fe II] 20F λ5006 + 4F λ5007	11	12
[Fe II] 18F λ5108 + 19F λ5112	2	...
[Fe II] 18F λ5158 + 19F λ5159	12	15
[N I] λ5198, λ5200	125	119
[Fe II] 18F λ5269, λ5273	11	15
[Fe II] 19F λ5334	3	4
[Fe II] 19F λ5376	2	3
[Fe II] 17F λ5413 + 16F λ5413	1	...
[Fe II] 17F λ5527	3	6
[O I] λ5577	7	10
[Fe I] 2F λ5696 ?	2	...
[N II] λ5755	7	12
He I λ5876	6	6
Na I λ5890, λ5896	5	6
[O I] λ6300	303	441
[O I] λ6363	99	137
[N II] λ6548	29	37
Hα λ6563	350	357
[N II] λ6584	81	115
He I λ6678	2	...
[S II] λ6717	64	68
[S II] λ6731	120	140

TABLE 2

EMISSION-LINE AND CONTINUUM POLARIZATION OF GL 618

	EAST LOBE		WEST LOBE	
ION	P (%)	θ (°)	P (%)	θ (°)
[O I]	3.5 ± 0.7	140 ± 6	3.0 ± 1.3	150 ± 13
[N I]	4.2 ± 1.1	131 ± 8	6.8 ± 4.8	136 ± 20
[N II]	2.1 ± 1.4	168 ± 19	3.8 ± 3.0	178 ± 23
[S II]	3.6 ± 1.0	140 ± 8	3.1 ± 2.4	119 ± 23
[Fe II]	5.6 ± 6.1	165	...	...
H I	13.1 ± 0.6	2 ± 1	7.0 ± 1.6	6 ± 7
He I	9.3 ± 5.6	8 ± 17	20 ± 10	26 ± 15
Forbidden lines	3.3 ± 0.5	140 ± 4	2.8 ± 1.0	147 ± 10
Permitted lines	13.0 ± 0.6	2 ± 1	7.2 ± 1.6	7 ± 2
Continuum	26.0 ± 0.3	2 ± 1	29.1 ± 1.5	174 ± 2

component would have the same polarization as the continuum. It is likely that an additional portion of the permitted-line radiation is emitted within the lobes themselves, and should be polarized like the forbidden lines. Since the degree and position angle of polarization of both components are known, it is straightforward to compute the fraction α_s, of scattered permitted-line radiation in this two-component model. The values of α_s so determined are:

$$\text{East lobe: } \alpha_s = 0.49 \pm 0.03 .$$

$$\text{West lobe: } \alpha_s = 0.21 \pm 0.07 .$$

With these scattered fractions, the observed permitted-line polarization and position angle measurements are reproduced to within the errors.

i) *The Central Nebula*

We have shown that a substantial fraction of the permitted-line radiation observed in each lobe originates in a central nebula hidden from our direct view. Since no such component is detected in any of the forbidden lines, we infer that the electron density in the central nebula is sufficient to collisionally depopulate the forbidden transitions. This implies $N_e \gtrsim 10^6$ cm^{-3}. We identify this region with the radio-continuum source detected by Wynn-Williams (1977). The self-absorbed spectrum between 5 and 15 GHz implies an emission measure greater than 10^9 pc cm^{-6}. A diameter near 0".15 is inferred from the flux density, so with our distance estimate the radio observations also yield $N_e \gtrsim 10^6$ cm^{-3}. The radio-frequency emission measure implies ~ 10 times more Balmer emission than is actually detected from the central nebula; the disparity is representative of scattering properties of the object. This central ionized nebula is presumably gas in the dense dusty torus.

ii) *Emission in the Lobes*

The peculiar emission-line spectrum of GL 618, which strongly favors the cooling lines of heavy elements, can now be attributed to the visible nebulae themselves. Conditions in the two lobes are evidently very unusual but remarkably similar: with the scattered fractions of H I emission deduced above, the intrinsic [O I] λ6300/Hβ intensity ratios are 5.9 and 5.6 for the east and west nebulae, respectively.

Diagrams of log N_e versus log T_e have been generated on the basis of the measured intensity ratios [O I] (λ6300 + λ6363)/λ5577, [S II] (λ6717 + λ6731)/(λ4068 + λ4076), [S II] λ6717/λ6731, and [N II] (λ6548 + λ6584)/λ5755. Calculations representing a five-level atom were used, with atomic constants by Czyzak *et al.* (1970) for [S II] and by MacAlpine (1971) for [O I] and [N II]. A high degree of stratification is indicated by the diagrams. The [O I] ratio implies a temperature in the neutral zone $T_e \approx 10{,}000$ K, while the corresponding electron density is limited by the great strength of [N I] λ5200, whose upper level becomes predominantly depopulated by collisions for $N_e \gtrsim 2 \times 10^3$ cm^{-3}. In the region producing emission from the first ionized states of the heavy elements, the density (as indicated by [S II] line ratios) exceeds 2×10^4 cm^{-3} and $T_e \approx 18{,}000$ K.

Volumetric filling factors for the various ions can be estimated from the observed line intensities and the emissivity in a collisionally excited transition:

$$4\pi j_{21} = N_e N_i \frac{8.63 \times 10^{-6} \Omega(1,2)}{T^{1/2} \omega_1} \times h\nu_{21} e^{-\chi/kT} \text{ ergs cm}^{-3} \text{ s}^{-1} . \quad (1)$$

Here N_i is the ionic density, $\Omega(1, 2)$ the collision strength, ω_1 the statistical weight of the lower level, and χ the excitation energy of the upper level, all in cgs units. For the ionized gas, we assume cosmic abundances and complete ionization of hydrogen, and $N_e = N_{H^+} = N_H \approx 5 \times 10^4$ cm^{-3}. Pressure equilibrium is assumed to exist between the two zones, so in the neutral gas $N_H \approx 10^5$ cm^{-3}, but $N_e = N_{H^+} \approx 10^3$ cm^{-3}. In both cases, the range of heavy-element ionization is assumed to be restricted to the single species observed. Collision strengths are as above. The computed filling factors show good agreement among the various ions existent in each zone, with

$$f(H^0) > 0.1 \text{ (D/1.8 kpc)}^{-1} ,$$
$$f(H^+) > 2 \times 10^{-3} \text{ (D/1.8 kpc)}^{-1} . \quad (2)$$

Inequalities result from the possibilities that an atom is in more than one ionization state and that we may have underestimated the line emission if significant absorption occurs within the nebulae. Due to the dependence of H^+ recombinations on N_e^2, the Balmer emission arises almost entirely within the ionized gas.

For the purpose of this discussion, we can therefore describe the lobes of GL 618 by a simple two-component model. The primary constituent is neutral gas with $T_e \approx 10^4$ K, $N_e \approx 10^3$ cm^{-3}, wherein emission from [O I], [N I], [C I], Mg I], and Na I originates. Since little stellar radiation with $h\nu > 7$ eV is present in this gas, it must be shielded from the starlight. The second component is hotter and contains hydrogen which is largely ionized, but fills a small fraction of the visible nebulae. Emission from H I, He I, [S II], [N II], and probably [Fe II] occurs in this gas, which is presumably subject to a relatively unattenuated stellar radiation field. The electron density in this zone is sufficiently high that the ^2D term of O^+ is primarily collisionally depopulated, hence the weakness of [O II] λ3727, but the $\lambda\lambda$7320, 7330 lines are prominent (Westbrook *et al.* 1975).

The strength of emission from low-ionization heavy elements has been a concern since the first serious attempts at a detailed understanding of PN shells were made. An excellent review of this subject is contained in Katz (1980). Briefly, lines from species such as [N I], [N II], [O I], and especially [O II] are observed to be overly intense compared with model calculations. An inclusion of charge-exchange reactions in the models has improved the situation somewhat (Williams 1973), and it has been suggested that dynamical effects may play a role (Shields 1978), but it appears that the best opportunity for reconciliation of the observations and theory lies in the existence of dense, neutral condensations in PN shells. Models of a nebula with such condensations were made by Williams (1970), while their formation through Rayleigh-Taylor instabilities at an ionization front was explored by Capriotti (1973). The effect that an optically thick condensation would have in shadowing the outlying nebula from ionizing flux was considered by Van Blerkom and Arny (1972). In this situation, the incident radiation field in a shadow is only the diffuse emission due to recombinations of H^+ to the ground state in the surrounding ionized gas. Van Blerkom and Arny assumed that the shadows themselves are optically thin to the diffuse field and obtained somewhat improved intensities for the low-ionization lines. Shadows which are optically thick were considered by Mathis (1976); however, he also noted that in dusty shells, scattering of

stellar UV photons throughout the nebula will tend to equalize the ionization states of shadowed and unshadowed zones, thereby removing some of the effect that shadows had in increasing the low-ionization flux.

A definite improvement in models including shadows has recently been presented in the calculations of Katz (1980). This work treats the problem in a self-consistent manner by allowing the shadowed regions to affect the thermal and ionization structures of the nebula. General features of the results include the shadows being cooler and in a lower level of ionization than the ambient nebula. The differences amount to factors of nearly two in temperature and ten in the degree of ionization of hydrogen, while the heavy elements in a shadow generally exist in the next lower stage of ionization. The predicted line intensity ratios agree rather well with the observations, with the relative prominence of low-ionization lines being determined primarily by the radial locations of condensations and the filling factor of the shadows.

On the basis of this information, we associate the ionized and neutral components of the lobes of GL 618 with unshadowed and shadowed material, respectively. The overall level of ionization in this object is lower than that in the aforementioned models due to the cooler central star ($\sim$ 30,000 K versus $\sim$ 100,000 K). Therefore, O is primarily O^+ in the unshadowed gas of GL 618 in contrast to O^{++} in normal PNs, and the shadows of GL 618 are primarily neutral, that is, in one stage of ionization lower than the unshadowed gas. The temperature in the shadows ($\sim$ 10,000 K) is also roughly one-half that of the ambient gas ($\sim$ 18,000 K), a result of the softer spectrum of diffuse emission as compared with the stellar radiation field. The ionized gas itself is hotter than a normal H II region due to its high density, which reduces the effectiveness of certain cooling lines (such as [O II] λ3727), and due to the compact ionized region near the star, which hardens the stellar spectrum through its considerable optical depth just above the Lyman limit.

The shadows considered by Katz (1980) and Van Blerkom and Arny (1972) are optically thin to the Lyman continuum. This situation results from rather basic assumptions of the physical conditions. Their nebula is taken to have characteristics of a typical PN, with a size $\sim 10^{18}$ cm and $N_e \approx 10^3$ cm^{-3}. The shadows themselves are therefore relatively highly ionized ($N_{H^0}/N_H \approx 10^{-2}$). In addition, the condensations are patterned after knots actually observed in nearby PNs (Capriotti, Cromwell, and Williams 1971), which have sizes $\approx 10^{15}$ cm. These parameters combine to yield transverse optical depths in a shadow of at most a few tenths at the Lyman limit. For the case of GL 618, the inferred neutral hydrogen density in a shadow is so high that large Lyman-continuum optical depths are encountered for dimensions down to $\sim 5 \times 10^{12}$ cm. This suggests that the shadows in GL 618 are optically thick, which would account for their very low state of ionization and for why the derived filling factors of neutral and ionized gas total less than unity. Therefore, in contrast to a normal PN shell, where shadows appear as narrow shafts of neutral gas behind dense knots, a picture more appropriate for GL 618 is one in which radial filaments of ionized material penetrate the nebula where the column density is sufficiently low. The required condensations are very likely associated with dust clouds near the star, perhaps in the dusty torus itself. A sketch of the physical structure envisioned for GL 618 is shown in Figure 2.

Heating of neutral gas surrounding an ionized filament occurs primarily through photoionization of hydrogen by a UV photon from the filament. This mechanism dominates over direct electron conduction, since it operates over a distance corresponding to the mean free path of a Lyman continuum photon, $\sim 10^{13}$ cm, versus $\sim 5 \times 10^{11}$ cm for conduction (Sage and Seaton 1973). The UV flux incident on the shadowed gas will in general contain two components: the diffuse radiation field due to ground-state recombinations of H^+ in the ionized filament, and stellar continuum photons scattered by dust grains in the lobe. For heating of the neutral gas solely by diffuse radiation, Hummer and Seaton (1973) have shown on quite general grounds that

$$N_e^2(H^0)V(H^0) < 0.6N_e^2(H^+)V(H^+) \qquad (3)$$

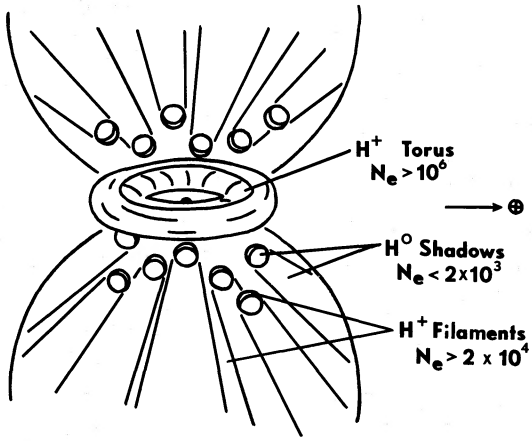

FIG. 2.—A sketch of the proposed structure of GL 618. The inner torus is ionized by intense starlight, but obscured in our direction by outlying dust. Neutral gas in the shadows of dense condensations fills most of the nebular volume. The Earth lies in the plane of the torus.

With the parameters derived for GL 618, this condition is easily satisfied.

A more stringent evaluation of the thermal balance can be made on the basis of the observed forbidden-line intensities. The primary cooling mechanism of the shadowed gas is collisional excitation followed by radiation of neutral atoms. Since H^0 excitation does not set in strongly until above $T = 10^4$ K, the lines [O I] $\lambda\lambda$6300, 6363, [C I] $\lambda\lambda$9823, 9849, and [N I] $\lambda\lambda$5198, 5200 carry most of the energy. The total luminosity contained in these and weaker observed features is the energy loss rate $L = 6.3 \times 10^{33}$ $(D/1.8 \text{ kpc})^2$ ergs s^{-1}. (The CO emission detected by Lo and Bechis 1976 presumably arises in the cold interiors of shadows but is insignificant in terms of cooling the nebula.) We compare the radiation losses with the gains, G, due to photoionization by the diffuse field. For complete absorption of this radiation by the neutral gas,

$$G = \alpha_1 N_e^2(H^+)V(H^+)\langle h\nu_D - \text{ryd}\rangle , \quad (4)$$

where α_1 is the ground-state recombination coefficient and $\langle h\nu_D - \text{ryd}\rangle$ is the mean excess energy of a diffuse photon above 1 rydberg. Since little of the observed Hβ flux originates within the shadows, we write in a similar fashion

$$4\pi D^2 F(H\beta) = \alpha_{H\beta}^{\text{eff}} N_e^2(H^+)V(H^+)h\nu_\beta . \quad (5)$$

Equation (5) is solved for N_e^2V and inserted into (4). Substitutions for the known quantities are then made, using our result that one-half of the observed Hβ flux is scattered from the central nebula and assuming $\langle h\nu_D - \text{ryd}\rangle = 3$ eV. We obtain $G \approx 3.2 \times 10^{33}$ $(D/1.8 \text{ kpc})^2$ ergs s^{-1}, about one-half that needed to offset the radiation losses. It is apparent from this result that scattered starlight must be a significant source of energy to the shadows as well. Given $\tau_{sca} \approx 0.03$ for the entire nebula in the visual (§ IIc), a substantial scattering optical thickness in the UV along a filament is quite plausible.

We have shown that the optical spectrum of GL 618 can be understood in a general manner by a model containing a two-phase composition for the visible nebulae plus a compact high-density core very near the star. The lobes are composed primarily of neutral gas of moderately high density, which is heated by diffuse emission and scattered stellar radiation from ionized filaments. Of course, more quantitative models akin to those of Katz (1980) should be developed before such a picture is accepted. However, several properties of the object suggest that a detailed understanding will be difficult to attain. For example, the high optical depths implied in the shadows necessitates the consideration of stratification near a shadow boundary, an effect ignored by Katz. Similarly, the generally unknown scattering and absorption characteristics of the dust (especially in the UV) are expected to be important factors.

Should the general picture outlined above prove to be inadequate, perhaps dynamical effects, such as recombination and cooling of material flowing into a shadow, should be considered. If the cooling time of infalling gas is shorter than the crossing time of a shadow, material may collect in cold shadow interiors and be shocked by subsequent inflow. Since apparently little ionization of hydrogen occurs, shock velocities would be restricted to less than ~ 50 km s^{-1}. For such velocities and condensations the size observed in classical PNs, a shock front might indeed be set up for a short time. Dopita (1978) has modeled the emission from low-velocity shocks with emphasis toward understanding the low-ionization Herbig-Haro (HH) objects. In fact, one such object, HH 47, exhibits an optical spectrum very similar to that of GL 618 with $I(\lambda(6300) \approx I(H\alpha)$ and lines of [N I], Mg I], and [Fe II] similarly enhanced (Dopita 1978; Böhm, Brugel, and Mannery 1980). Unfortunately, the gas density in GL 618 is at least two orders of magnitude greater than that inferred for HH 47, and the model of HH 47 itself is extremely crude, so the shock hypothesis is difficult to evaluate in any detail. Potential problems with such a mechanism for GL 618 include the large fraction of the visible nebulae currently emitting in the neutral forbidden lines, and the lack of evidence for any mass motions greater than 20 km s^{-1}.

It is important to note, however, that the general features inferred to exist in GL 618 (i.e., condensations, shadows) are observed in normal PNs. The greater relative importance of these phenomena in the bipolar nebula presumably points to its less evolved state.

III. M2-9

The nearly symmetric bipolar nebula M2-9 has received a great deal of attention in recent years owing to its peculiar appearance and spectral characteristics. On photographs (Allen and Swings 1972), the object consists of a bright central core bracketed by two more diffuse nebulosities $\sim 10''$ to the north and south. The "wings" are highlighted by bright condensations which vary in appearance on time scales as short as a few years (van den Bergh 1974), most likely due to changes in illumination by a central star. A strong near-infrared continuum originating within 3″ of the center was detected by Allen and Swings. Data were extended to 18 μm by Cohen and Barlow (1974), who conclude that a substantial amount of dust ranging in temperature from 450 to 830 K is present. Optical spectra of the central nebula and lobes have been presented by Allen and Swings (1972), Calvet and Cohen (1978), and Swings and Andrillat (1979). A rather weak ratio continuum has been observed (Purton, Feldman, and Marsh 1975); however, as yet, attempts at detecting molecular radio emission have failed (Zuckerman *et al.* 1977).

a) Observations

An image tube photograph taken by E. A. Harlan on the Lick 1.0 m Nickel telescope reveals that the morphology of the lobes in 1980 May was accented by four partially resolved knots, located 15″ S, 1″ E; 12″ S, 4″ E; 9″ N, 4″ E; and 14″ N of the central nebula. ITS spectrophotometry and spetropolarimetry were obtained of the core and of all but the southernmost condensation during the period 1979 June–1980 July. Generally, complete

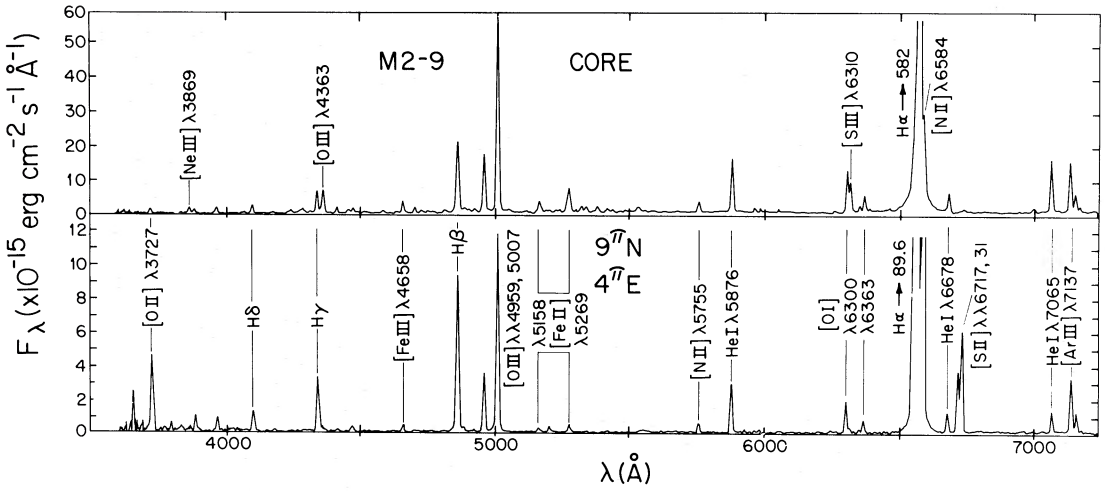

FIG. 3.—Observed flux spectra of the central core of M2-9 and a representative knot in the lobes, located 9″ N, 4″ E of the star.

coverage of the wavelength range 3750–7050 Å was obtained using apertures of 2″.8 or 4″.0, depending upon the atmospheric seeing.

Representative spectra are shown in Figure 3. The knots all exhibit very similar characteristics, with strong lines of H I, He I, [O III], [O II], [O I], [N II], and [S II], plus weaker [Fe II], [N I], and [S III]. In the central nebula Hα is exceedingly strong, but lines of He I, [O III], and [Fe II] also stand out and [S II], [N II], [Fe III], [Ne III], [O I], and Si II are present. Quantitatively, the observed line strengths are in good agreement with earlier spectrophotometry by Calvet and Cohen (1978) and Swings and Andrillat (1979). On the basis of the observed Balmer decrements and the standard reddening law, the previous values of $A_v = 2.7$ mag and ~ 5 mag are confirmed for the visual extinction toward the lobes and the central core, respectively (however, in § III*b* we show that the Balmer lines in the lobes are largely scattered, so $A_v = 2.7$ mag may be an underestimate of the true extinction here). A weak continuum is present at each location.

Table 3 summarizes the polarimetry by ion for each nebulosity. Substantial polarization is present in the lobes, and, as in GL 618, large differences exist in the properties of various ions. Previous spectropolarimetry of the core of M2-9 (Calvet and Cohen 1978) found a position angle of 65°, near the 76° reported in Table 3, but a much higher degree of polarization. The new data are considered much more reliable, since the present instrument is not subject to the systematic effects of changes in atmospheric transparency and seeing or guiding and centering errors. The new data confirm the similar polarizations of the emission lines and continuum in the core.

The extensive tabulations of Mathewson and Ford (1970) reveal that, for stars near M2-9 ($l^{II} = 11°$, $b^{II} = +18°$) which suffer more than ~ 2 mag of visual extinction, the interstellar polarization is substantial ($P \approx 4\%$, $\theta \approx 90°$). The rough agreement between these values and our measurements of the central nebula suggests that an interstellar component may be dominating the polarization of the core light. Support for this view includes (1) the close similarity between the emission-line and continuum polarizations in the core, (2) a quite flat $P(\lambda)$ curve between 4000 Å and 7000 Å for the core, and (3) an inferred extinction of $A_v \approx 2.7$ mag for each knot in the lobes. We will take the overall polarization of the core ($P = 3.6\%$, $\theta = 76°$) as the interstellar component in this direction.

In the lower portion of Table 3 are listed the mean polarizations of the emission lines and continuum with the assumed interstellar component subtracted. Of importance here is a comparison between the intrinsic position angle of polarization for each spectral component and the corresponding entry in the bottom row, which is the position angle of a perpendicular to the radius vector drawn from the central core. The very good agreement implies that the intrinsic polarization of the lobes arises via scattering of light emitted near the star and further substantiates our choice of the interstellar polarization toward M2-9.

b) Geometry of the Emission Regions

Complications arise when estimating the scattered fractions of emission-line flux in the lobes due to the fact that the intrinsic polarization of scattered light is not known. Unlike GL 618, the continuum in M2-9 is not entirely scattered starlight, but contains a substantial component due to hydrogen continuum emission (Calvet and Cohen 1978), which may originate locally or be scattered. However, limits can be set on the scattered fractions by assuming that the polarization of a scattered component alone (1) must at least equal that of the local continuum, but (2) does not exceed the values found in the most highly polarized bipolars ($\sim 50\%$). The results (Table 4) reveal that scattering has a considerable influence on the spectrum of the lobes in M2-9.

i) *The Central Nebula*

It is evident from Table 4 that $\sim 60\%$ of the permitted-line radiation observed in the lobes is scattered in our direction after being emitted in the core, whereas only

TABLE 3

EMISSION-LINE AND CONTINUUM POLARIZATION OF M2-9

	NEBULOSITY							
	12″ S, 4″ E		9″ N, 4″ E		14″ N		Central Core	
ION	P (%)	θ (°)	P (%)	θ (°)	P (%)	θ (°)	P (%)	θ (°)
[O I]	3.1 ± 2.0	94 ± 18	5.0 ± 2.9	92 ± 16	16.6 ± 6.4	149 ± 11	2.9 ± 0.8	68 ± 8
[O III]	6.8 ± 1.0	74 ± 4	5.4 ± 1.2	88 ± 6	6.1 ± 1.2	81 ± 6	4.3 ± 0.5	70 ± 3
[N II]	6.2 ± 0.5	75 ± 2	6.1 ± 0.6	87 ± 3	5.0 ± 0.7	84 ± 4	...	...
[S II]	8.6 ± 3.1	76 ± 10	6.9 ± 3.8	68 ± 16	6.2 ± 2.3	79 ± 11	...	...
H I	19.8 ± 0.4	71 ± 1	16.7 ± 0.5	105 ± 1	8.4 ± 0.6	85 ± 2	3.4 ± 0.1	77 ± 1
He I	8.9 ± 3.6	78 ± 12	15.4 ± 5.5	92 ± 10	5.9 ± 3.0	78 ± 15	3.4 ± 0.9	77 ± 8
Forbidden lines	6.2 ± 0.4	75 ± 2	5.9 ± 0.5	87 ± 3	5.2 ± 0.6	83 ± 3	3.9 ± 0.4	70 ± 3
Permitted lines	19.7 ± 0.4	71 ± 1	16.7 ± 0.5	105 ± 1	8.3 ± 0.6	85 ± 2	3.4 ± 0.1	77 ± 1
Continuum	20.1 ± 0.7	70 ± 1	20.4 ± 0.9	108 ± 1	12.2 ± 1.0	86 ± 2	4.9 ± 0.3	75 ± 2
Interstellar Component Subtracted								
Forbidden lines	2.6 ± 0.5	74 ± 6	2.9 ± 0.5	101 ± 5	1.9 ± 0.6	97 ± 9	...	...
Permitted lines	16.2 ± 0.5	70 ± 1	15.1 ± 0.5	111 ± 1	5.0 ± 0.6	91 ± 3	...	...
Continuum	16.6 ± 0.7	69 ± 1	19.1 ± 0.9	113 ± 1	8.9 ± 1.0	90 ± 3	...	...
Perpendicular to star	...	72 ± 3	...	114 ± 3	...	90 ± 3	...	...

~ 10% of the observed forbidden-line emission follows this route. The flux ratio of a forbidden line to Hβ in the incident spectrum is therefore $\sim \frac{1}{6}$ that measured in the lobes. For [O III] λ5007, this implies a strength relative to Hβ of only ~ 1:5. The comparative weakness of forbidden lines in the central nebula suggests that, as in GL 618, the electron density is sufficiently high ($N_e \gtrsim 10^6$ cm^{-3}) to collisionally depopulate the forbidden transitions.

The absolute core emission-line flux incident on grains in the lobes, F_i, can be estimated from

$$F_i \approx \frac{4\alpha_s F_L}{\tau_s \Theta_k^2}, \tag{6}$$

where F_L is the dereddened line flux we observe in the lobe, α_s is the appropriate scattered fraction from Table 4, τ_s is the scattering optical depth, and Θ_k is the apparent angular radius of the knot. We have no knowledge of τ_s, but can obtain a lower limit to F_i by assuming $\tau_s = 1$, since the scattered spectrum strengthens more slowly than τ_s for larger optical depths. Substituting values appropriate for the knots in M2-9, we find

$$F_i(\mathrm{H}\beta) \gtrsim 0.1 \text{ ergs cm}^{-2} \text{ s}^{-1},$$
$$F_i(\lambda 5007) \gtrsim 0.02 \text{ ergs cm}^{-2} \text{ s}^{-1},$$

which correspond to core luminosities of

$$L_i(\mathrm{H}\beta) \gtrsim 6 \times 10^{34} (D/1 \text{ kpc})^2 \text{ ergs s}^{-1},$$
$$L_i(\lambda 5007) \gtrsim 1 \times 10^{34} (D/1 \text{ kpc})^2 \text{ ergs s}^{-1}.$$

(We have followed Calvet and Cohen 1978 in assuming a distance to M2-9 of 1 kpc.)

We compare this inferred spectrum of the core *as seen by the lobes* with that emitted in our direction. After making a reddening correction corresponding to $A_v = 5$ mag, the observed line ratios of [O I], [O III], [S II], and [N II] all confirm the high electron density ($N_e \gtrsim 10^6$ cm^{-3}). The absolute emission-line luminosities implied by our core measurements amount to

$$L(\mathrm{H}\beta) \approx 1.5 \times 10^{34} (D/1 \text{ kpc})^2 \text{ ergs s}^{-1},$$
$$L(\lambda 5007) \approx 2.7 \times 10^{34} (D/1 \text{ kpc})^2 \text{ ergs s}^{-1}.$$

Thus, we can account for the scattered forbidden-line radiation as being the observed core emission which reaches the lobes relatively unattenuated. However, the observed Hβ flux falls short by a factor of at least 4 in producing the scattered spectrum of the lobes. We conclude that the spectrum of the central core as seen by the lobes is quite different from that observed from our perspective. Evidently, a large amount of Balmer emission arises very near the star and escapes freely into the polar lobes but is absorbed in our direction by the dusty torus. In this context, it is interesting to consider the anomalously large Hα/Hβ ratio (~ 27) observed in the core. Calvet and Cohen (1978) attributed the measurement of the effects of Balmer self-absorption, which is quite plausible for the densities present. However, if the ratio is taken at face value, a visual extinction of ~ 6.5 mag is implied. When this larger value of A_v is included in

TABLE 4

SCATTERED FRACTIONS IN THE LOBES OF M2-9

	KNOT		
LINE	12″ S, 4″ E	9″ N, 4″ E	14″ N
Forbidden lines	0.05–0.16	0.06–0.15	0.04–0.21
Permitted lines	0.32–0.98	0.30–0.79	0.10–0.56

the above calculations, adequate Balmer emission is present in the core to produce the scattered spectrum. In any event, the conclusion of a high degree of obscuration in our direction but a relatively clear path to the lobes confirms that the nebulosities we see are polar lobes situated above and below a flattened torus rather than a large ring seen edge-on. The $\pm 15\,\mathrm{km\,s^{-1}}$ radial velocities observed in the lobes (Allen and Swings 1972) therefore represent expansion of the object.

ii) *Emission in the Lobes*

A two-phase composition for the lobes of M2-9 was inferred from radio continuum measurements (Purton, Feldman, and Marsh 1975) and reaffirmed by inspection of the optical forbidden-line spectrum (Calvert and Cohen 1978). Since the scattered fractions of these features are now known to be small, we can be certain that the forbidden-line spectrum is representative of conditions in the lobes themselves. Using the atomic parameters described in § IIc(ii), we find that both [N II] and [S II] arise in a zone with $N_e \approx 10^4\ \mathrm{cm^{-3}}$, $T_e \approx 9000$ K. From the absolute intensities of these lines and of [O II], the filling factor is $\gtrsim 0.1$, and one can show that most of the Balmer emission intrinsic to the lobes arises here as well. The lines of [O III] and [O I], on the other hand, indicate a slightly hotter region where $N_e \approx 10^6\ \mathrm{cm^{-3}}$. The filling factor of this zone is uncertain, since the primary ionization state of oxygen, the density indicator, is unknown. However, if O is distributed equally over the first three stages of ionization, then $f \approx 10^{-6}$. If O^+ is the primary constituent, then $f \lesssim 10^{-5}$ in order for the accompanying Balmer emission not to exceed that observed. Emission from [O II], [S II], and [N II] is suppressed in this zone by collisional de-excitation.

The picture which emerges is one very similar to that in GL 618, where a low-ionization medium filling most of the volume is accompanied by gas of much higher N_e and higher ionization, but low filling factor. The temperature in the zone of high N_e is closer to normal in M2-9 due to its higher ionization state, which enables efficient coolants such as [O III] $\lambda\lambda$4959, 5007. Evidently, this gas is exposed to a harder stellar radiation field, so it is very likely situated near the inner boundary of a knot. The lines of [O I] $\lambda\lambda$6300, 6363 may be enhanced through charge-exchange reactions of O^+ with neutral H (Williams 1973).

VI. DISCUSSION

Combined spectrophotometry and spectropolarimetry have permitted us to deduce the structure and emission geometry of GL 618 and M2-9. Both objects can be represented by the now-familiar model of a pair of polar lobes situated above and below a dense dusty torus which is heated by the central star. A compact, very high-density central nebula, probably gas in the torus itself, produces intense Balmer emission which is observed after scattering off dust in the lobes. The lobes themselves have a two-phase composition: a low-ionization, ambient gas of moderate electron density which fills most of the volume, plus more highly ionized, rather sparse zones of much higher N_e. From both observational and theoretical points of view, these bipolar nebulae therefore fit naturally into present conceptions of the initial development of planetary nebulae. In particular, the presence of condensations, shadows which emit strongly in forbidden-line radiation, and large quantities of dust are predicted by many models of young PNs. For distances near those assumed, linear dimensions of the visible nebulae are ~ 0.05 pc (GL 618) and ~ 0.15 pc (M2-9), compact by comparison with normal PNs (~ 0.1–0.7 pc). Masses in the lobes lie in the range 0.02–0.1 $M_\odot$, so that together with the torus material, nebular masses typical of the shells of Population I PNs ($\sim 0.2\ M_\odot$) are probably present.

Both GL 618 and M2-9 are located near the beginning of the theoretical sequence of PN nuclei (Calvet and Cohen 1978) which occurs when the star becomes hot enough to ionize the nebula a few thousand years after mass ejection from the red giant (Härm and Schwarzschild 1975). A somewhat more advanced stage is suggested for M2-9 by its higher degree of ionization (therefore hotter star) and larger size. In fact, this is confirmed by estimates of nebular ages using the observed sizes and expansion velocities. Ignoring projection effects, the radial velocity difference of $30\,\mathrm{km\,s^{-1}}$ between the lobes of M2-9 indicates mass ejection occurred ~ 5000 years ago. The CO emission-line width of GL 618 suggests an age near 1500 years.

The physical conditions in a very young PN are conducive to the formation not only of dust and dense condensations of atomic gas, but also of molecules. Grains which condense in the cool ejecta soon after release from the stellar surface serve to shield outer material from the stellar UV and act as condensation sites for molecules such as H_2. In an atmosphere rich in carbon, CO will also be abundant. A search for very young PNs using a CO emission criterion has been successful (Zuckerman 1978; Zuckerman *et al.* 1977, 1978); their list of candidates includes several well-known carbon stars and bipolar nebulae. On the other hand, CO emission is observed near other (e.g., young) objects as well, while some proto–PNs may be missed in CO surveys due to a low abundance of carbon or a particular stage of evolution not characterized by strong molecular emission. In particular, we have shown that GL 618 and M2-9 have a common physical structure which is expected for proto–PNs; however, only GL 618 is detected in CO. The most likely explanation for this result lies in the evolutionary difference between the two objects. The vast regions of cool, neutral gas in GL 618 are optically thick in the UV and therefore provide an environment favorable to the existence of molecules. The corresponding ambient gas in M2-9 is singly ionized, implying a strong ultraviolet radiation field and gas temperature $\sim 10{,}000$ K—both of which would destroy CO.

It therefore appears that the identification of proto–PNs must rely on a variety of data, and that searches for emission from molecular species other than CO would be advisable. In this context it is interesting to note the lack of CO emission but a detection of the OH radical in the

bipolar nebula M1-92 (Lépine and Nguyen-Quang-Rieu 1974).

The authors thank J. S. Miller and L. V. Kuhi for donations of observing time on the 3 m telescope. Valuable discussions were held with W. Mathews, D. E. Osterbrock, T. Jones, and H. Liszt. We are also grateful to E. A. Harlan, who provided a photograph of M2-9, and to R. Antonucci for aid with the data reduction. Support was provided through NSF grant AST 78-19753, grants from the University of Minnesota Office of Academic Affairs and Institute of Technology (G.S.), and the National Research Council through an NAS/NRC Senior Postdoctoral Resident Research Associateship at NASA Ames Research Center (M.C.).

REFERENCES

Allen, D. A., and Swings, J. P. 1972, *Ap. J.*, **174**, 583.
Böhm, K. H., Brugel, E. W., and Mannery, E. 1980. *Ap. J.* (*Letters*), **235**, L137.
Calvet, N., and Cohen, M. 1978, *M.N.R.A.S.*, **182**, 687.
Capriotti, E. 1973, *Ap. J.*, **179**, 495.
Capriotti, E. R., Cromwell, R. H., and Williams, R. E. 1971, *Ap. Letters*, **7**, 241.
Cohen, M., and Barlow, M. J. 1974, *Ap. J.*, **193**, 401.
Czyzak, S. J., Krueger, T. K., Martins, P. de A. P., Saraph, H. E., and Seaton, M. J. 1970, *M.N.R.A.S.*, **148**, 361.
Dopita, M. A. 1978, *Ap. J. Suppl.*, **37**, 117.
Gottlieb, E. W., and Liller, Wm. 1976, *Ap. J.* (*Letters*), **207**, L135.
Härm, R., and Schwarzschild, M. 1975, *Ap. J.*, **200**, 324.
Herbig, G. H. 1975, *Ap. J.*, **200**, 1.
Hummer, D. G., and Seaton, M. J. 1973, *Mém. Soc. Roy. Sci. Liège, 6th Ser.*, **5**, 245.
Kaler, J. B. 1978, *Ap. J.*, **220**, 887.
Katz, A. 1980, preprint.
Kleinmann, S. G., Sargent, D. G., Moseley, H., Harper, D. A., Loewenstein, R. F., Telesco, C. M., and Thronson, H. A., Jr. 1978, *Astr. Ap.*, **65**, 139.
Lépine, J. R. D., and Nguyen-Quang-Rieu. 1974, *Astr. Ap.*, **36**, 469.
Lo, K. Y., and Bechis, K. P. 1976, *Ap. J.* (*Letters*), **205**, L21.
MacAlpine, G. A. 1971, Ph.D. thesis, University of Wisconsin.
Mathewson, D. S., and Ford, V. L. 1970, *Mem. R.A.S.*, **74**, 139.
Mathis, J. S. 1976, *Ap. J.*, **207**, 442.
Miller, J. S., and Mathews, W. G. 1972, *Ap. J.*, **172**, 593.
Miller, J. S., Robinson, L. B., and Schmidt, G. D. 1980, *Pub. A.S.P.*, **92**, 702.
Ney, E. P., Merrill, K. M., Becklin, E. E., Neugebauer, G. and Wynn-Williams, C. G. 1975, *Ap. J.* (*Letters*), **198**, L129.
Osterbrock, D. E. 1974, *Astrophysics of Gaseous Nebulae* (San Francisco: Freeman).
Purton, C. R., Feldman, P. A., and Marsh, K. A. 1975, *Ap. J.*, **195**, 479.
Sage, G., and Seaton, M. J. 1973, *Mém. Soc. Roy. Sci. Liège, 6th Ser.*, **5**, 241.
Salpeter, E. E. 1971, *Ann. Rev. Astr. Ap.*, **9**, 127.
Schmidt, G. D., Angel, J. R. P., and Beaver, E. A. 1978, *Ap. J.*, **219**, 477.
Shields, G. 1978, *Ap. J.*, **219**, 565.
Stone, R. P. S. 1977, *Ap. J.*, **218**, 767.
Swings, J. P., and Andrillat, Y. 1979, *Astr. Ap.*, **74**, 85.
Van Blerkom, D., and Arny, T. T. 1972, *M.N.R.A.S.*, **156**, 91.
van den Bergh, S. 1974, *Astr. Ap.*, **32**, 351.
Westbrook, W. E., Becklin, E. E., Merrill, K. M., Neugebauer, G., Schmidt, M., Willner, S. P., and Wynn-Williams, C. G. 1975, *Ap. J.*, **202**, 407.
Williams, R. E. 1970, *Ap. J.*, **159**, 829.
———. 1973, *M.N.R.A.S.*, **164**, 111.
Wynn-Williams, C. G. 1977, *M.N.R.A.S.*, **181**, 61P.
Zuckerman, B. 1978, in *IAU Symposium 76, Planetary Nebulae*, ed. Y. Terzian (Dordrecht: Reidel), p. 305.
Zuckerman, B., Palmer, P., Gilra, D. P., Turner, B. E., and Morris, M. 1978, *Ap. J.* (*Letters*), **220**, L53.
Zuckerman, B., Palmer, P., Morris, M., Turner, B. E., Gilra, D. P., Bowers, P. F., and Gilmore, W. 1977, *Ap. J.* (*Letters*), **211**, L97.

MARTIN COHEN: NASA Ames Research Center, Mailstop 245-6, Moffett Field, CA 94035

GARY D. SCHMIDT: School of Physics and Astronomy, Tate Laboratory of Physics, University of Minnesota, 116 Church Street S.E., Minneapolis, MN 55455